The iron ligand sphere geometry of mammalian 15-lipoxygenases

Ralf Jürgen KUBAN*, Rainer WIESNER*, Jörg RATHMAN*, Gerrit VELDINK†, Hans NOLTING‡, V. A. SOLÉ‡ and Hartmut KÜHN*[1]

*Institute of Biochemistry, University Clinics Charité, Humboldt University, Hessische Str. 3-4, D-10115 Berlin, Germany, †Bijvoet Center for Biomolecular Research, Department of Bio-organic Chemistry, Utrecht University, Padualaan 8, NL-3584 CH Utrecht, The Netherlands, and ‡EMBL Outstation, c/o Deutsches Elektronen Synchrotron DESY, Notkestraße 4, Hamburg, Germany

We investigated the geometry of the iron ligand sphere of the native rabbit 15-lipoxygenase (15-LOX) by X-ray absorption spectroscopy using synchrotron radiation. The soybean LOX-1 was used as a reference compound because its iron ligand sphere is well characterized. For structural information the X-ray absorption spectra were evaluated using the Excurve Program (CCLRC Daresbury Laboratory, Warrington, U.K.). From the positions of the absorption edges and from the intensities of the 1s–3d pre-edge transition peaks a six-coordinate ferrous iron was concluded for the rabbit 15-LOX. Evaluation of the extended region of the absorption spectra suggested six nitrogen and/or oxygen atoms as direct iron ligands, and the following binding distances were determined (means ± S.D.; estimated accuracy is ± 0.001 nm for bond distances, on the basis of more than 22 X-ray absorption spectra): 0.213 ± 0.001 nm, 0.213 ± 0.001 nm, 0.236 ± 0.001 nm, 0.293 ± 0.001 nm, 0.189 ± 0.001 nm and 0.242 ± 0.001. Lyophilization of the LOX altered the binding distances but did not destroy the octahedral iron ligand sphere. For construction of a structural model of the iron ligand sphere the binding distances extracted from the X-ray spectra were assigned to specific amino acids (His-360, -365, -540, -544 and the C-terminal Ile-662) by molecular modelling using the crystal coordinates of the soybean LOX-1 and of a rabbit 15-LOX–inhibitor complex.

INTRODUCTION

Lipoxygenases (LOXs) are lipid-peroxidizing enzymes which occur in plants and in animal cells [1,2]. According to the currently used nomenclature, which is based on the positional specificity of arachidonic acid oxygenation, three major types of mammalian LOXs may be differentiated: 5-LOXs, 12-LOXs and 15-LOXs. The 5-LOXs are key enzymes in the biosynthesis of leukotrienes, which are mediators of anaphylactic and inflammatory reactions [3]. 15-LOXs have been implicated in the maturational breakdown of mitochondria during red blood cell maturation [4]. The observation that a functional 15-LOX is expressed at a high level in foamy macrophages of atherosclerotic lesions [5–7] suggested a pathophysiological role of the enzyme in atherogenesis. Recently, it was shown that a 15-LOX inhibitor which does not lower plasma cholesterol levels appeared to protect from the development of atherosclerotic lesions in cholesterol-fed rabbits [8], suggesting a pro-atherogenic action of the enzyme. Thus, LOXs may constitute a pharmacological target for the development of potential anti-atherosclerotic drugs, substituting for lipid lowering therapy.

For a rational drug design direct structural data on mammalian LOXs are required. However, at this point of research, structural information on mammalian LOXs is rather limited. Studies of the CD as well as evaluation of the 1s–3d transition pre-edge signal in the X-ray absorption spectrum revealed that mammalian 15-LOXs in their non-activated ground state contain six-coordinate ferrous iron [9]. Site-directed mutagenesis studies on various mammalian LOXs [10–12] suggested four histidines and the C-terminal isoleucine as iron-liganding amino acids. This suggestion is supported by recent X-ray crystallographic data on a rabbit 15-LOX–inhibitor complex [13]. In addition to these experimental data, there are computer-generated models for certain features of the structure of mammalian LOXs [14] that are based on the X-ray coordinates of the plant LOXs [15–18]. In contrast to the mammalian enzymes there is a substantial body of structural information on plant LOXs. X-ray investigations of soybean LOX-1 crystals at a resolution of 2.6 Å suggested a four-coordinate non-haem iron [15]. Simultaneous X-ray investigations of soybean LOX-1 crystals by other authors suggested a five-coordinate iron ligand sphere with a vacant sixth ligand position [16]. In addition to His-499, His-504, His-690 and Ile-839, the δ oxygen of Asn-694 was identified as an iron ligand. Later crystallographic studies, at a resolution of 1.4 Å, indicated that a water molecule may occupy the sixth ligand position [16,17]. The more recently published crystal structure of the soybean LOX-3 also suggested a six-coordinate iron [18]. In addition to the crystallographic data, there are a number of spectroscopic studies aimed at defining the geometric and electronic structure of the iron environment. Investigations of the magnetic susceptibility [19] suggested that the ferrous active site ground state is high-spin, with $S = 2$. Measurements of the X-ray absorption [20,21], Mössbauer spectroscopy [22] and experiments on the magnetic CD [23] predicted a distorted octahedral iron ligand sphere. A recent CD/magnetic CD study suggested that the soybean LOX-1 may exist as a 40:60 mixture of five- and six-coordinate forms and turn into a purely six-coordinate species after addition of alcohols or fatty acids [9].

In order to obtain direct structural information on the geometry of the iron ligand sphere of mammalian LOXs we carried out X-ray absorption studies on the native rabbit reticulocyte 15-LOX. The data obtained suggested the presence ferrous non-haem iron in a distorted octahedral ligand sphere. Six nitrogen and/or oxygen atoms may act as direct iron ligands, surrounding the central atom in a distance of 0.189 ± 0.001 nm to 0.293 ± 0.001 nm (means ± S.D.; estimated accuracy is ± 0.001 nm for bond distances, on the basis of more than 22 X-ray absorption spectra).

Abbreviation used: LOX(s), lipoxygenase(s).

[1] To whom correspondence should be addressed (e-mail hartmut.kuehn@rz.hu-berlin.de).

EXPERIMENTAL

Preparations

The soybean LOX (isoenzyme-1) was purified to electrophoretic homogeneity from natural sources (Williams soybeans, American Quality B) as described previously [19]. The enzyme preparation exhibited a catalytic-centre activity with respect to linoleic acid of about 300 s^{-1}. After the final preparation step the buffer was changed to a 50 mM Bistris-buffer, pH 6.8, and the enzyme was concentrated using a collodion bag micro-concentrator (Sartorius, Gottingen, Germany) to a final concentration of 82 mg/ml. Precipitates formed during the concentration procedure were spun down.

The rabbit reticulocyte LOX was prepared to apparent homogeneity from the lysate of a reticulocyte-rich blood-cell suspension by fractionated ammonium sulphate precipitation and consecutive hydrophobic interaction and anion-exchange chromatography [24]. The final enzyme preparation exhibited a catalytic-centre activity with respect to linoleic acid of 30 s^{-1}. An iron content of 0.95 g-atom of iron/mol of enzyme was determined by atomic absorption spectroscopy. The buffer of the enzyme preparation was changed to a 50 mM Bistris buffer, pH 6.8, using Bio-Rad desalting columns, and the enzyme was concentrated to a final protein concentration of about 35 mg/ml as described for the soybean enzyme. We noticed that further concentration of the enzyme was accompanied by a precipitation of the protein and an impaired specific activity. Before transferring the enzyme solution to the measuring cell the precipitate formed during concentration was removed by centrifugation. For measurements of the lyophilized enzyme the buffer of the enzyme preparation was changed to a volatile ammonium bicarbonate buffer (10 mM, pH 7.4) and this solution was lyophilized overnight.

X-ray absorption measurements

The concentrated enzyme solutions and the lyophilized protein were transferred to a home-made plastic cell (1 mm in thickness), the measuring windows of which were covered by a Kapton (Dupont, Dusseldorf, Germany) membrane. The samples were frozen in liquid nitrogen and stored at -80 °C until measurement. X-ray absorption studies were carried out using the EMBL (European Molecular Biology Laboratory) X-ray absorption spectrometer [25,26] at HASYLAB (c/o Deutsches Elektronen Synchrotron, Hamburg, Germany). An Si(III) double-crystal monochromator with an energy resolution of 1.9 eV (DE) at 7250 eV (E), resulting in a $DE/E = 2.6 \times 10^{-4}$, was used. The second monochromator crystal was detuned to 50 % in order to reject harmonics of higher order. The monochromator angle was converted to an absolute energy scale by applying a calibration technique [26], resulting in an accuracy better than 0.2 eV. The 15-LOX X-ray absorption spectra were recorded by monitoring the X-ray fluorescence of the samples with a 13-element germanium solid-state detector. A series of 22–55 spectra were taken for each sample at 20 K. The spectra were recorded in the range 6900–7900 eV with steps of 0.3 eV in the near-edge region. No evident damage of the protein sample occurred during the exposure to the X-ray beam, as far as can be judged from the identity of the first and the last spectra collected.

Data evaluation and statistics

The fluorescence raw data obtained during X-ray absorption measurements were reduced using computer programs developed at the EMBL outstation. Determination of the intensities of the pre-edge 1s–3d transition peak was carried out as described earlier [27]. Reference values for the intensity of this peak have been reported previously for low-molecular-mass model ferrous compounds [9]. Evaluation of the EXAFS spectra was carried out with the Excurve Program (version 92, CCLRC Daresbury Laboratory, Warrington, U.K.). In the first step of the evaluation process a theoretical EXAFS spectrum for the ferrous soybean LOX was constructed which was based on the coordinates of the iron ligands obtained during X-ray investigations of LOX-1 crystals at a resolution of 2.6 Å [15]. In the second step the theoretical spectrum was fitted stepwise to the measured EXAFS spectra by varying the coordinates of the atoms surrounding the central iron at a distance of up to 0.45 nm. These variations did not allow major distortions of the imidazole rings of the histidine residues. The quality of fitting represented by the R value was calculated from 500 data points over the entire measuring range. The R factor is defined by the following equation:

$$R = \sum_{i}^{N} (1/\sigma_i)\,(|\chi^{\exp}(k_i) - \chi^{\mathrm{the}}(k_i)|)\,100\,\%$$

in which $\chi^{\exp}(k_i)$ represents the experimental EXAFS data and $\chi^{\mathrm{the}}(k_i)$ the calculated data. The $(1/\sigma_i)$ weighting term is defined by:

$$1/\sigma_i = k_i^n \Big/ \sum_{j}^{N} k_j^n [\chi_j^{\exp}(k_j)]$$

in which N represents the number of data points and n a number chosen so that the term $k_j^n[\chi_j^{\exp}(k_j)]$ has an approximately constant amplitude over the entire data range. For biological molecules an R factor of 15 % indicates good agreement of experimentally obtained traces and the calculated data. In contrast, an R value of 40 % or higher indicates poor fitting.

Amino acid alignment of the mammalian LOXs and the soybean enzyme suggested that Asn-694, which is an iron ligand in the soybean enzyme, is substituted for a histidine in the human and rabbit 15-LOXs [14]. Thus we replaced, on the computer, the asparagine by a histidine, keeping the coordinates of the polypeptide backbone unchanged. Then the imidazole ring of this histidine was allowed to twist around the Cβ–Cγ-axis, reaching the thermodynamically most favourable configuration. Afterwards, a theoretical EXAFS spectrum of this computer-generated mutant was constructed and the model spectrum was fitted to our experimental EXAFS data of the rabbit 15-LOXs by varying the binding distances of the iron ligands.

	499				504			690				694			839		
soybean 15-lipoxygenase	S	**H**	W	L	N	T	**H**	A	A	L	**H**	A	A	V	**N**	F	I	S	**I**
human 15-lipoxygenase	S	**H**	L	L	R	G	**H**	L	M	Q	**H**	A	S	V	**H**	L	V	A	**I**
human 5-lipoxygenase	T	**H**	L	L	R	T	**H**	L	V	Q	**H**	A	A	V	**N**	**F**	V	A	**I**
porcine 12-lipoxygenase	S	**H**	L	L	R	G	**H**	L	M	Q	**H**	S	S	N	**H**	L	V	A	**I**
mouse 12-lipoxygenase	A	**H**	L	L	R	G	**H**	L	V	Q	**H**	S	S	I	**H**	L	V	A	**I**
rabbit 15-lipoxygenase	S	**H**	L	L	R	G	**H**	L	M	Q	**H**	S	S	I	**H**	L	V	A	**I**
	360				365			540				544			662		

Figure 1 Alignment of amino acid sequences of various LOXs containing the direct iron ligands

The one letter code for amino acids is used and the iron ligand amino acids are marked in bold face. The numberings of the amino acids for the soybean enzyme (above the alignment) and for the rabbit enzyme (below the alignment) are given. Large gaps indicate that these parts of the primary structure are distant from each other in the overall amino acid sequence.

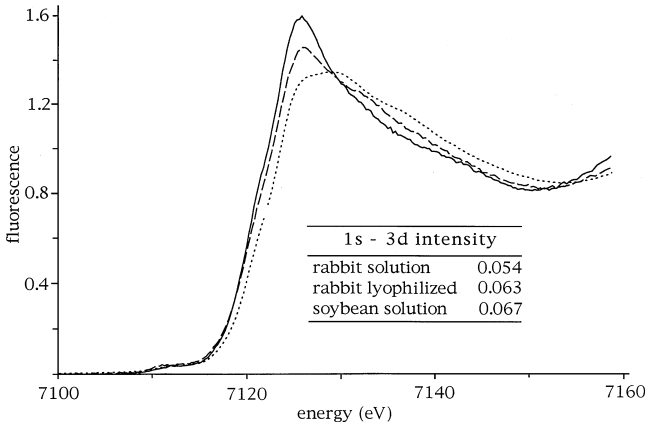

Figure 2 Normalized near-edge region of the X-ray absorption spectra of 15-LOXs

Preparation of the enzymes and X-ray absorption spectroscopy were as described in the Experimental section. Solid line, solution of rabbit LOX, dotted line, lyophilized rabbit lipoxygenase; broken line, solution of soybean LOX. The normalized intensities of the 1s–3d pre-edge transition peaks are given in the inset.

RESULTS

X-ray absorption studies

Plant and mammalian LOXs share a high degree of amino acid identity in the central region of their primary structures, particularly in the environment of the putative iron ligands (Figure 1). Since the soybean LOX-1 is well characterized with respect to the geometry of its iron ligand sphere we used this enzyme as a reference compound for X-ray absorption studies on the rabbit reticulocyte 15-LOX. Comparison of the edge-position in the X-ray absorption spectra (Figure 2) indicated the presence of ferrous iron in both plant and animal LOXs. The intensities of the pre-edge 1s–3d transition signals of the normalized spectra (inset) revealed that the soybean and the rabbit enzymes contain six-coordinate iron.

In Figure 3, the X-ray absorption spectra (weighted fine structure k^3 and phase-corrected Fourier transforms) for the solutions of the soybean LOX-1 and the rabbit 15-LOX, as well as the corresponding data for the lyophilized rabbit enzyme, are shown. In all cases a good agreement between the computer-simulated model spectra (red traces) and our experimental data (yellow traces) was observed (R values ranging between 8.1 % and 14.8 %). If one compares directly the absorption spectra of the rabbit and the soybean LOXs (Figure 4) clear differences can be seen. These differences may be due not only to different binding distances of the iron ligands but also to the fact that the chemistry of the iron ligands may be different. As indicated in Figure 1, Asn-694 of the soybean enzyme is aligned with His-544 of mammalian 15-LOXs, suggesting that this histidine residue may function as an iron ligand in these enzymes. Evaluation of the extended region of the X-ray absorption spectra of the soybean LOX-1 suggested six nitrogen and/or oxygen atoms as direct iron ligands, and the following binding distances were determined (means $\pm$ S.D.): 0.214 $\pm$ 0.001 nm, 0.215 $\pm$ 0.001 nm, 0.215 $\pm$ 0.001 nm, 0.304 $\pm$ 0.001 nm, 0.195 $\pm$ 0.001 nm and 0.247 $\pm$ 0.001 nm. It should be mentioned that when evaluating the extended region of the X-ray absorption spectra we were not able to discriminate between five- and six-coordinate enzyme species. In both cases the quality of data fitting was comparable (R = 11.3 % for five-coordinate compared with 11.4 % for six-coordinate). However, the intensities of the pre-edge 1s–3d transition signals (Figure 2) suggested mainly a six-coordinate iron, and these data are in line with earlier reports on the iron ligand sphere geometry of this enzyme [9]. The X-ray absorption spectra of the rabbit reticulocyte 15-LOX (in solution) also suggested six nitrogen and/or oxygen atoms as direct iron ligands, and for this enzyme the following binding distances were calculated (means $\pm$ S.D.): 0.213 $\pm$ 0.001 nm, 0.213 $\pm$ 0.001 nm, 0.236 $\pm$ 0.001 nm, 0.293 $\pm$ 0.001 nm, 0.189 $\pm$ 0.001 nm and 0.242 $\pm$ 0.001 nm. As for the soybean enzyme, no difference in the quality of fitting was observed when a five- or six-coordinate iron was assumed. Here again, the evaluation of the 1s–3d pre-edge transition peak suggested six-coordinate iron. This result is in line with an earlier conclusion drawn from other spectroscopic studies [9]. The lyophilized rabbit enzyme also contains six-coordinate ferrous iron, as suggested by the intensity of the 1s–3d pre-edge transition peak. If water is considered to be a direct ligand, as was shown for the soybean LOX [17], it appears not to be removed during the lyophilization process. However, the

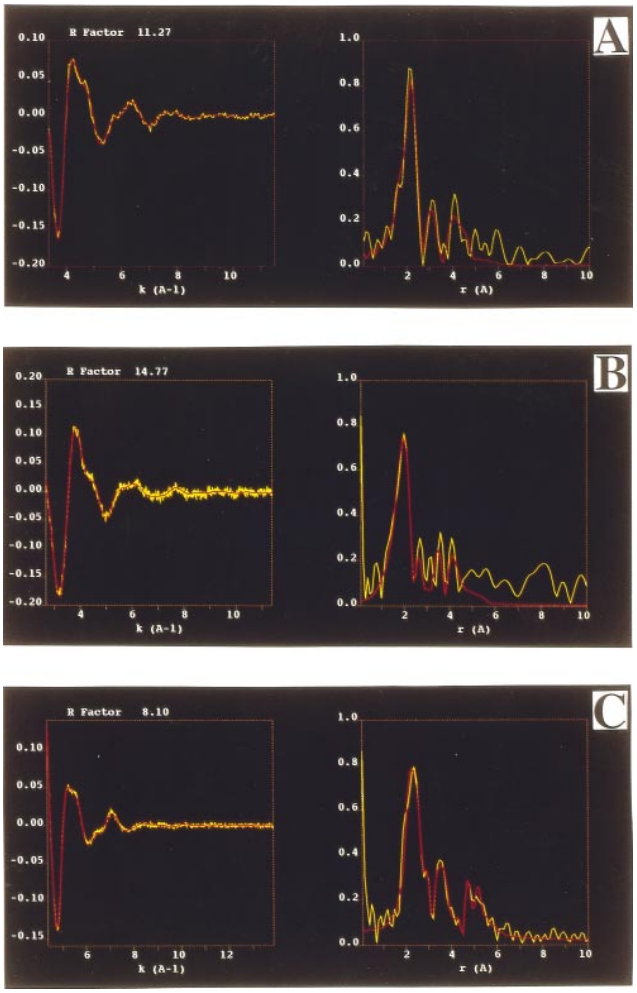

Figure 3 X-ray absorption spectra of 15-LOXs

The weighted fine structure k^3 (left side) and the phase-corrected Fourier transforms (right side) of 15-LOXs are shown. Theoretical spectra (red lines) are superimposed by the experimental data (yellow lines). For calculation of the model spectra the atoms surrounding the central iron at a distance of less than 0.45 nm were considered. (**A**) Solution of soybean LOX; (**B**), solution of rabbit LOX; (**C**), lyophilized rabbit LOX.

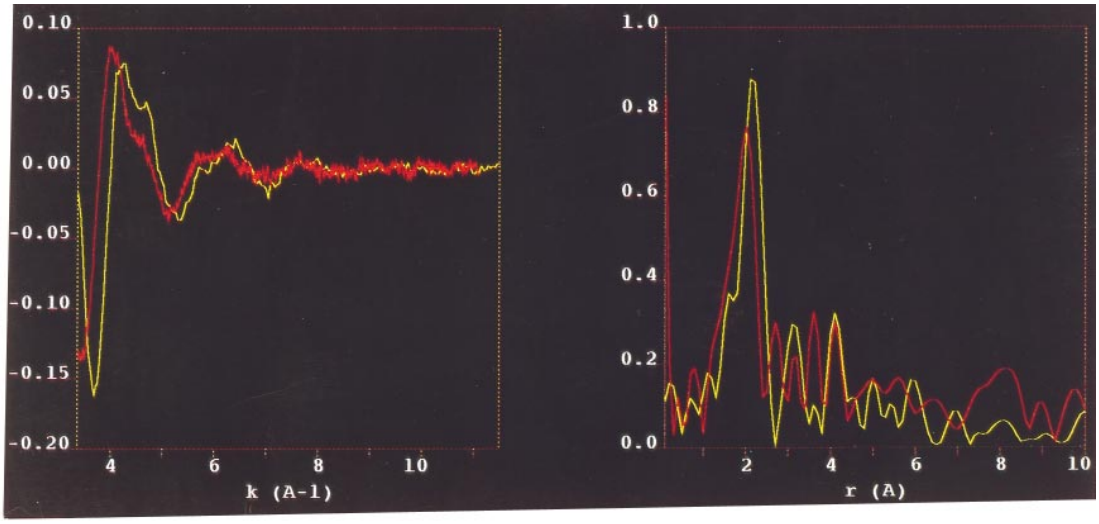

Figure 4 Comparison of the X-ray absorption spectra of the rabbit and soybean 15-LOXs

The weighted fine structure k^3 (left side) and the Fourier transforms (right side) of the X-ray absorption spectra are shown. The spectra were taken for concentrated solutions (pH 6.8) of the soybean LOX (yellow trace) and the rabbit 15-LOX (red trace).

Table 1 Binding distances of the direct iron ligands of LOXs

Mean values are given for the EXAFS data. Standard deviations of our EXAFS data are given in parentheses [(1) is equivalent to 0.001 nm]. It should be stressed that the assignment which bonding distance goes with which ligand is based on our EXAFS results, on the crystallographic data obtained for the soybean LOX and computer-assisted structural modelling.

Crystallographic data				EXAFS data					
Soybean LOX-1 (PDB entry 2SBL)*		Soybean LOX-1 ref. [17]†		Soybean LOX-1 (solution) This paper ($R = 11.3\%$)		Rabbit LOX (solution) This paper ($R = 15.3\%$)		Rabbit LOX (lyophilized) This paper ($R = 8.1\%$)	
Ligand	Distance (nm)	Ligand	Distance (nm)	Ligand	Distance (nm)	Ligand	Distance (nm)	Ligand	Distance (nm)
His-499 Nϵ2	0.227	His-499 Nϵ2	0.223	His-499 Nϵ2	0.214 (1)	His-360 Nϵ2	0.213 (1)	His-360 Nϵ2	0.265 (1)
His-504 Nϵ2	0.222	His-504 Nϵ2	0.226	His-504 Nϵ2	0.215 (1)	His-365 Nϵ2	0.213 (1)	His-365 Nϵ2	0.225 (1)
His-690 Nϵ2	0.225	His-690 Nϵ2	0.221	His-690 Nϵ2	0.215 (1)	His-540 Nϵ2	0.236 (1)	His-540 Nϵ2	0.244 (1)
Asn-694 Oδ1	0.316	Asn-694 Oδ1	0.305	Asn-694 Oδ1	0.304 (1)	His-544 Nδ1	0.293 (1)	His-544 Nδ1	0.308 (1)
Ile-839 O1	0.216	Ile-839 O1	0.240	Ile-839 O1	0.195 (1)	Ile-662 O1	0.189 (1)	Ile-662 O1	0.192 (1)
Water O			0.256		0.247 (1)		0.242 (1)		0.208 (1)

* Root mean square deviation of bond lengths, 0.0012 nm.
† Geometric deviations of bond lengths, 0.0011 nm.

binding distances of the iron ligands were altered upon lyophilization (0.265 ± 0.001 nm, 0.225 ± 0.001 nm, 0.244 ± 0.001 nm, 0.308 ± 0.001 nm, 0.192 ± 0.001 nm and 0.208 ± 0.001 nm).

Molecular modelling of the iron ligand sphere

From the EXAFS spectra it was concluded that six nitrogen and/or oxygen atoms constitute the direct iron ligands in plant and animal LOXs. Earlier X-ray analysis of soybean LOX-1 crystals identified the ϵ-nitrogen atoms of His-499, -504, -690, the δ1 oxygen of Asn-694, a carboxylic oxygen of the C-terminal Ile-839 and a water molecule as iron ligands [17]. For mammalian LOXs mutagenesis studies indicated four histidines and the C-terminal isoleucine as iron ligands, and multiple sequence alignments (Figure 1) suggested that His-360, -365, -540 and -544 and Ile-662 may function as iron-liganding amino acids in the rabbit 15-LOX. In order to assign the binding distances calculated from the X-ray absorption spectra to specific amino acid residues molecular modelling was carried out. For this purpose we used the coordinates for the soybean LOX-1 crystals [15] and assumed that the iron ligand sphere of the rabbit enzyme may be similar to that of the soybean LOX-1, with the exception of the Asn-694 $\rightarrow$ His-544 exchange (Figure 1). During the modelling procedure we found that the δ1-nitrogen of His-544 appeared to be the direct iron ligand. This finding was somewhat surprising, since for the other histidines (His-360, -365 and -540) the ϵ2-nitrogen constitutes the liganding atom. In order to substantiate this finding the imidazole ring of His-544 was rotated on the computer in steps of 10° around the Cβ–Cγ axis. For each configuration the distances of the δ- and of the ϵ-nitrogens to the central iron were determined. In the best fits (R 14.8 %) the distances of the δ- and ϵ-nitrogens to the iron were 0.293 ± 0.001 nm and 0.435 ± 0.001 nm respectively (means $\pm$ S.D.). Using this method, a minimal Fe^{2+}–Nϵ2 distance of

0.385 nm was reached, but the R value of this fit was more than 10% higher than for the optimal fit, suggesting that the ϵ2-nitrogen may not constitute the direct iron ligand. We also rotated the histidine side-chain around the Cα–Cβ axis, but noticed that the histidine nitrogens quickly moved out of the iron ligand sphere. Thus, for our modelling studies we kept the orientation of the Cα–Cβ bond as it was in the crystallographic measurements of the soybean LOX-1. The recently published coordinates of the rabbit 15-LOX–inhibitor complex also suggest that the δ-nitrogen of His-544 is the direct iron ligand [13].

In Table 1 the results of our combined X-ray absorption and molecular modelling studies are compared with previously reported crystallographic measurements. For the soybean LOX-1 the binding distances calculated from the crystallographic experiments were consistently somewhat shorter than those extracted from our EXAFS spectra. A similar difference was noticed when earlier EXAFS data were compared with the 1.4 Å resolution crystal structure [17], although the reasons for this phenomenon remain unclear.

DISCUSSION

Since the publication of two independent crystal structures for the iron environment of the soybean LOX-1 in 1993 [15,16], the structure of the iron ligand sphere of LOXs has been a matter of discussion. The most significant difference between the two crystal structures was the function of Asn-694. Boyington et al. [15] suggested that the non-haem iron was four-coordinate, with His-449, -504, -690 and the C-terminal Ile-839 as iron ligands. Asn-694 was suggested to hydrogen-bond to a neighbouring glycine and thus may not be regarded as an iron ligand [15]. In contrast, Minor et al. [16] concluded from their electron-intensity map the existence of five direct protein iron ligands (His-499, -505, -690, -Ile839 and Asn-694) which may be arranged in a distorted octahedral ligand sphere with a vacant sixth position [16]. This position appeared to open into a cavity which may constitute the substrate-binding cleft. In a recent X-ray diffraction study at 1.4 Å resolution, a water molecule was identified as the sixth iron ligand [17]. Our data on the quantification of the pre-edge 1s–3d transition signal also suggested a six-coordinate iron, whereas evaluation of the fine structure of the spectrum's extended region could not discriminate between 5- and 6-coordinate forms. However, assuming a four-coordinate iron, with Asn-694 not being a direct ligand, the accuracy of fitting was lower, confirming that Asn-694 may act as an iron ligand in the soybean enzyme.

For mammalian LOXs a purely six-coordinate non-haem iron has been concluded from earlier CD measurements and from X-ray absorption studies in the near-edge region [9]. This conclusion was confirmed in our study. Summarizing the structural data on the iron ligand spheres of both plant and mammalian LOXs one may conclude that the ferrous iron in the native enzymes is six-

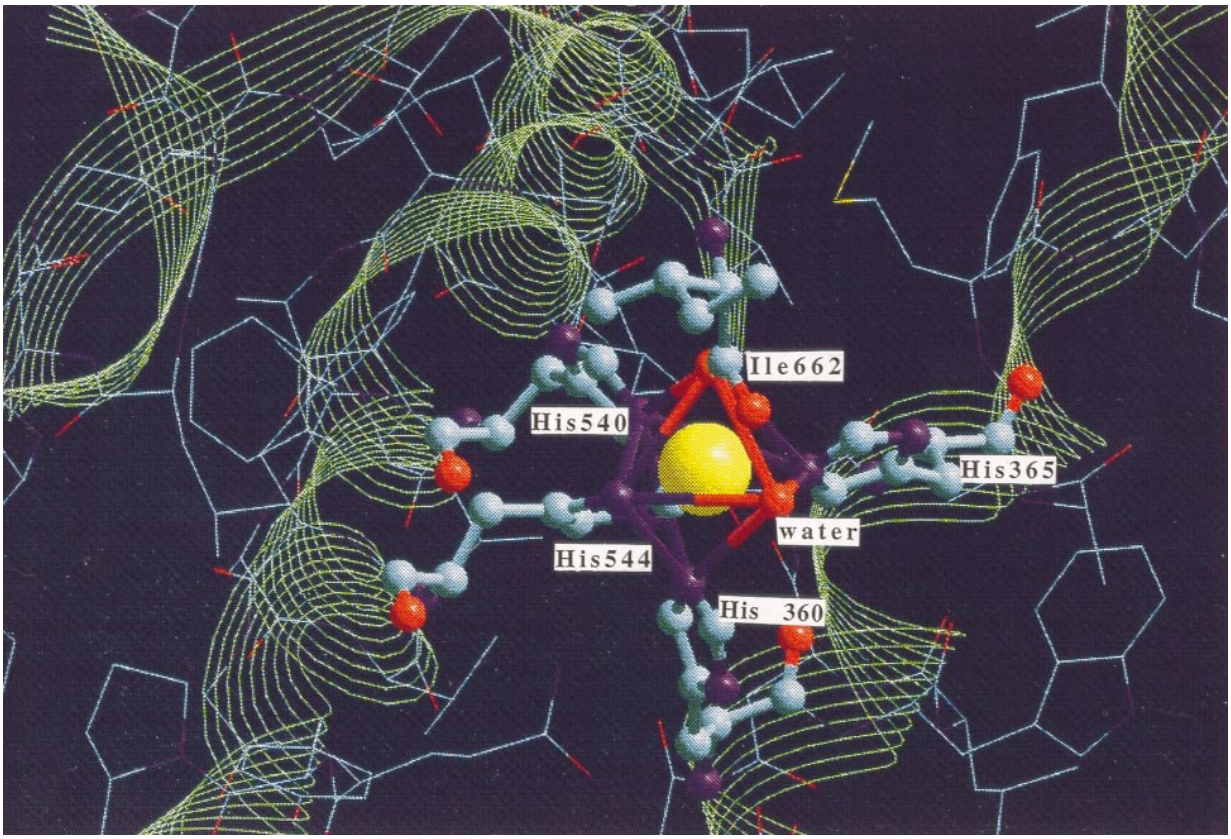

Figure 5 Octahedral iron ligand sphere of the rabbit 15-LOXs

The polypeptide backbone containing the C-terminal Ile-662 and the helices in which the iron-liganding histidines are located are indicated in green. The central iron is marked in yellow and the direct iron-liganding atoms are indicated in red (oxygens) and blue (nitrogens). The side-chains of liganding amino acids are also shown. It should be stressed that this model of the iron ligand sphere is not solely based on our EXAFS data, but is a result of molecular modelling using the X-ray coordinates of the soybean LOX-1 [15] and also takes into consideration the results of previous mutagenesis studies [10–12].

coordinate with five protein ligands and a water molecule occupying the sixth position. The ligand sphere can be described as a distorted bipyramid (octahedron). For the rabbit 15-LOX (Figure 5) His-365, His-540, His-544 and the water molecule constitute the edges of the octahedron's ground square, whereas His-360 and the C-terminal Ile-662 determine its longitudinal axis. The iron ligands His-360 and His-365 are parts of a long helix which spans almost the entire enzyme molecule [13]. This leading helix also contains Phe-353, which was recently identified as the primary determinant for the positional specificity of 12- and 15-LOXs [28]. It was suggested earlier that fatty acid substrates may displace the water molecule from the sixth ligand position [17]. In fact, such a displacement has been shown for a LOX inhibitor in the crystallographic studies of the rabbit 15-LOX–inhibitor complex [13]. It should be noted that, due to the binding forces of the central iron, the structure of this leading helix is disturbed between the two iron ligands [13]. His-540 and His-544, which constitute adjacent corners of the octahedron's ground square, are parts of another helix. Here again the helical structure may be disturbed between the iron ligands.

After lyophilization of the enzyme we observed significant changes in the edge position and in the weighted fine structure. These changes may, at least in part, be due to the fact that a part of the enzyme is oxidized to a ferric form during the workup procedure. However, this oxidation may not influence the enzyme activity, since LOXs shuttle between a ferrous and a ferric form during the catalytic cycle. When the lyophilized enzyme preparation was re-dissolved, it was found to be enzymically active. Moreover, we did not observe major alterations in the positional specificity of arachidonic acid oxygenation, suggesting that the absorption spectra had been taken from a native enzyme species. Evaluation of the EXAFS data of the lyophilized enzyme indicated that the binding distances of two direct iron ligands were modified, but the water molecule acting as sixth iron ligand was not removed (Table 1). Thus the overall structure of the octahedral ligand sphere appears to be retained. This result is of particular importance for further EXAFS studies on the rabbit LOX, which may be difficult to carry out with enzyme solutions because we have experienced problems with concentrating the enzyme.

Financial support for this study was provided by the Deutsche Forschungsgemeinschaft (grant Ku 961-2/1) and by the European Commission (CT 93-1790). We are greatly indepted to Dr. M. Browner (Rouche Bioscience, Palo Alto, CA, U.S.A.) who provided the X-ray coordinates of the rabbit 15-LOX–inhibitor complex.

Received 10 April 1997/19 January 1998; accepted 10 February 1998

REFERENCES

1 Nelson, M. J. and Seitz, S. T. (1994) Curr. Opin. Struct. Biol. **4**, 878–884
2 Yamamoto, S. (1992) Biochim. Biophys. Acta **1128**, 117–131
3 Lewis, R. A. and Austen, A. F. (1990) N. Engl. J. Med. **323**, 645–655
4 Rapoport, S. M., Schewe, T. and Thiele, B. J. (1990) Blood Cell Biochemistry **1**, 151–194
5 Kühn, H., Belkner, J., Zaiss, S., Fährenklemper, T. and Wohlfeil, S. (1994) J. Exp. Med. **179**, 1903–1911
6 Yla-Herttuala, S., Rosenfeld, M. E., Parthasarathy, S., Glass, C. K., Sigal, E., Sarkioia, T., Witztum, J. T. and Steinberg, D. (1991) J. Clin. Invest. **87**, 1146–1152
7 Folcik, V. A., Nivar-Aristy, R. A., Krajewski, L. P. and Cathcardt, M. K. (1995) J. Clin. Invest. **96**, 504–510
8 Sendobry, S. M., Cornicelli, J. A., Welch, K., Tait, B., Trivedi, B. K., Colbry, N., Dyer, R. D., Feinmark, S. J. and Daugherty, A. (1998) Br. J. Pharmacol. **120**, in the press
9 Pavlosky, M. A., Zhang, Y., Westre, T. E., Gan, Q. F., Pavel, E., Campochiaro, C., Hedman, B., Hodgson, K. O. and Solomon, E. I. (1995) J. Am. Chem. Soc. **117**, 4316–4327
10 Hammarberg, T., Zhang, Y. Y., Lind, B., Radmark, O. and Samuelsson, B. (1995) Eur. J. Biochem. **230**, 401–407
11 Suzuki, H., Kishimoto, K., Yoshimoto, T., Yamamoto, S., Kanai, F., Ebina, Y., Miyatake, A. and Tanabe, T. (1994) Biochim. Biophys. Acta **1210**, 308–316
12 Chen, X. S., Kurre, U., Copeland, N. G. and Funk, C. D. (1994) J. Biol. Chem. **296**, 13979–13987
13 Gillmor, S. A., Villasenor, A., Fletterick, R., Sigal, E. and Browner, M. F. (1997) Nature Struct. Biol. **4**, 1003–1009
14 Prigge, S. T., Boyington, J. C., Gaffney, B. J. and Amzel, L. M. (1996) Proteins **24**, 275–291
15 Boyington, J. C., Gaffney, B. J. and Amzel, L. M. (1993) Science **260**, 1482–1486
16 Minor, W., Steczko, J., Bolin, J. T., Otwinowski, Z. and Axelrod, B. (1993) Biochemistry **32**, 6320–6323
17 Minor, W., Steczko, J., Stec, B., Otwinowski, Z., Bolin, J. T., Walter, R. and Axelrod, B. (1996) Biochemistry **35**, 10687–10701
18 Skrzypczak-Jankun, E., Amzel, L. M., Kroa, B. A. and Funk, Jr., M. O. (1997) Proteins **29**, 15–31
19 Petersson, L., Slappendel, S. and Vliegenthart, J. F. G. (1985) Biochim. Biophys. Acta **828**, 81–85
20 van der Heijdt, L. M., Feiters, M. C., Navaratnam, S., Nolting, H. F., Hermes, C., Veldink, G. A. and Vliegenthart, J. F. G. (1992) Eur. J. Biochem. **207**, 793–802
21 Scarrow, R. C., Trimitsis, M. G., Buck, C. P., Grove, G. N., Cowling, R. A. and Nelson, M. J. (1994) Biochemistry **33**, 15023–15035
22 Dunham, W. R., Carroll, R. T., Thompson, J. F., Sands, R. H. and Funk, M. O. (1994) Eur. J. Biochem. **190**, 611–617
23 Whittaker, J. W. and Solomon, E. I. (1988) J. Am. Chem. Soc. **110**, 5329–5339
24 Belkner, J., Wiesner, R., Rathman, J., Barnett, J., Sigal, E. and Kühn, H. (1993) Eur. J. Biochem. **213**, 251–261
25 Hermes, C., Gilberg, E. and Koch, M. H. J. (1984) Nucl. Instrum. Methods **222**, 207–214
26 Pettifer, R. F. and Hermes, C. (1985) J. Appl. Crystallogr. **18**, 404–412
27 Bertini, I., Briganti, F., Mangani, S., Nolting, H. F. and Scozafava, A. (1994) Biochemistry **33**, 10777–10784
28 Borngräber, S., Kuban, R. J., Anton, M. and Kühn, H. (1996) J. Mol. Biol. **264**, 1145–1153